Validation of Large-scale Propagation Characteristics for UAVs within Urban Environment

Bucur, Madalina-Cristina; Sørensen, Troels Bundgaard; Amorim, Rafhael Medeiros de; Lechuga, Melisa Maria Lopez; Kovács, Istvan; E. Mogensen, Preben

Published in:
2019 IEEE 90th Vehicular Technology Conference (VTC2019-Fall)

DOI (link to publication from Publisher):
10.1109/VTCFall.2019.8891422

Publication date:
2019

Document Version
Accepted author manuscript, peer reviewed version

Validation of Large-scale Propagation Characteristics for UAVs within Urban Environment

Mădălina Bucur*, Troels B. Sørensen*, Rafhael Amorim*, Melisa Lopez*, Istvan Z. Kovács†, Preben Mogensen*†
*Department of Electronic Systems, Aalborg University, Denmark
{mcb, tbs, rma, mll, pm}@es.aau.dk
†Nokia Bell Labs, Aalborg, Denmark
{istvan.kovacs, preben.mogensen}@nokia-bell-labs.com

***Abstract*—Cellular networks based on current LTE Advanced or coming 5G technology, constitute an attractive candidate to provide communication links for drones in low level airspace. This paper extends previous findings on path loss exponent and shadow fading variation for an urban environment, by adding new and more extensive empirical evidence. Specifically, by way of the measurement methodology we study also the spatial correlation of the shadow fading, including the lateral spatial autocorrelation (decorrelation distance) and the cross-correlation in shadowing variability between different heights. Data was obtained with the use of a drone flying at heights up to and above rooftop, using a radio network scanner for measuring live LTE signals at 1800 MHz. The path loss analysis confirmed the validity of previously presented modelling frameworks for the behaviour versus height, as well as the characteristics of the increased interference observed when the drone is above rooftop level. As for the spatial correlation of the shadow fading, the results indicate that decorrelation distance does not change appreciably from ground level up to and above rooftop level, and remains in the order of 10m. The shadow fading variability is generally uncorrelated versus height, although with a trend to be correlated below rooftop level, but not above.**

I. Introduction

Unmanned Aerial Vehicles (UAVs), and drones more specifically, have been predicted big potential in many commercial applications and operations. It is considered that drone applications will create economic growth and new business opportunities, and considerable effort is devoted to the development of supporting technologies that would realize this potential, e.g. in the frame of the Single European Sky ATM Research (SESAR) *U-space* vision for drone integration with manned aviation [1]. For example, in this vision, the current constraints set by the requirement for Visual-Line-Of-Sight (VLOS) between the pilot and drone throughout the flight, can be relieved for many applications in the Very Low Level (VLL) airspace below approximately 150 meters. A prerequisite for this is that a reliable Command and Control (C2) datalink is established between the drone control (pilot in command), whether human or machine, for providing navigation commands, telemetry data and configuration and assistance for sense and avoid. As discussed in [2], cellular networks based on current LTE Advanced, or coming 5G technology, constitute an attractive candidate for C2 communication. The 3rd Generation Partnership Project (3GPP) recently concluded a study item on *"Enhanced LTE support for aerial vehicles"* [3], showing that this is already in the planning.

In order to understand the feasibility of providing drone C2 communication over the cellular network, a study on the wireless channel between the drone and existing Base Station (BS) infrastructure is required. Current cellular network deployments are optimized for coverage of users on or close to the ground, and to control the Inter-Cell Interference (ICI) between radio cells belonging to different BSs. In an urban scenario, it is expected that a drone will experience significant changes in the radio environment as it takes off close to ground level and into VLL airspace. At altitudes above building heights the UAV will benefit from radio clearance to multiple candidate BSs due to Line-Of-Sight (LOS) propagation [2], [4]. As a consequence of bandwidth reuse in cellular networks, unfortunately, the increased number of visible neighbour cells will also increase the interference seen by both the drone and the network.

The 3GPP Radio Layer WG1 (RAN1) has produced systematic measurements and modelling of UAV to ground channels, which enhances the previously proposed models [5]. Our recent work in [6] recommended a height dependent path loss model based on a number of field measurements in urban environment, and have similar behaviour to the 3GPP models. The field measurements were conducted in practical LTE network deployments, by measuring the LTE reference signals at varying heights up to 40m in a number of different locations (in a few cases up to 120m). The resulting model expresses the height dependence of the path loss versus distance (path loss slope) and the expected variability (standard deviation) of the path loss around its local distance dependent mean. The latter is often referred to as the shadow fading, although the exact definition depends on the scale of analysis, as it will become evident later in the paper. In the context of [6], the model expresses variability as seen over a larger urban area (large-scale shadowing).

The contribution in this paper is to bring further experimental evidence to the validity of the model in [6], by analysing more extensive and independent measurements from a similar, but different urban environment. A total of 41 different locations, covering complete street segments, were investigated at heights from 10 to 40m. In each case, the

scenario covered propagation paths towards multiple BS cells within the urban environment. Moreover, and in addition to previous literature, our measurement methodology provided for a study of the spatial correlation of the local shadow fading, including the lateral spatial autocorrelation (decorrelation distance) and cross-correlation between different heights. Our interest in this is to understand, eventually, the potential implications for the drone radio mobility performance, e.g. by modelling the shadowing variability for simulation studies.

The remainder of the paper is structured according to the following outline: Section II presents the urban scenario, the measurement setup and the methodology used for the processing of the measurement data. Section III is divided into three sets of results. First overall propagation characteristics, including ensemble statistics for the local shadowing, then interference statistics, and last the spatial correlation properties. Conclusions are given in Section V.

II. Measurement Setup and Data Processing

An extensive measurement campaign was carried out in August 2018, in the city of Aarhus, Denmark. The city covers an area of 91 $km^2$and has a population density of 3.000 pr. km^2 (2018)[1]. For the campaign, three different areas were selected as being representative of urban environment, ensuring some homogeneity in building layout and characteristics between them. Information regarding the chosen areas can be found in Table I, along with relevant network design parameters such as average BS antenna height and downtilt. Most buildings in the measurement areas have a gable roof construction, with the rooftop level starting some 4 to 5m below the top of the building. The antenna height and downtilt are essential parameters for ground user coverage optimization and ICI control. All BSs in the city area use the standard three-sector configuration with individual sectors, or cells, distributed by approximately 120 degrees in azimuth. Details on the network configuration were provided by courtesy of the Danish mobile operators.

In this measurement campaign, as in the one described in [6], the measurement equipment consisted of a Rohde & Schwarz TSME radio network scanner. The device was set to measure two carrier frequencies within the 1800 MHz band, belonging to two different Danish operators. The information reported by the scanner contains primarily the measured Reference Signal Received Power (RSRP) and Reference Signal

TABLE I: Characteristics of the measurement area; average BS height includes terrain height.

Area	Avg. building height [m]	Avg. ground level [m]	Avg. BS height [m]	Avg. antenna downtilt [degrees]	
				Operator 1	Operator 2
#1	13	6.95	28.3	5.6	5.2
#2	15	2.40	31.9	5.6	5.2
#3	19	0.12	31.7	5.6	5.2

[1]http://www.statistikbanken.dk/

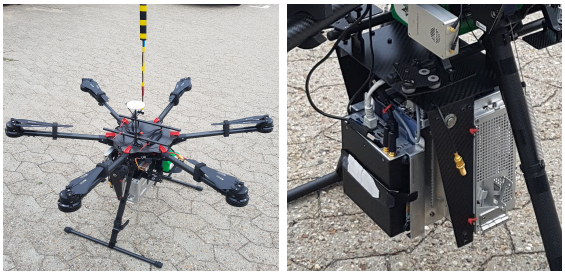

Fig. 1: a) S1000 drone with dipole antenna mounted 50cm above the drone carbon frame (left). b) Details of the measurement equipment mount underneath the drone (right).

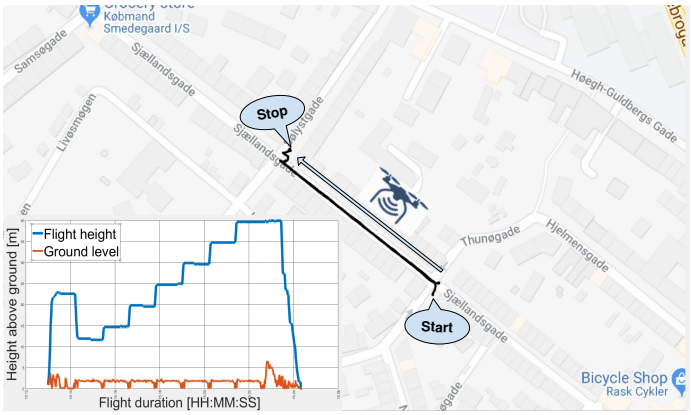

Fig. 2: Drone flying path and flight overview.

Received Quality (RSRQ) of the corresponding BS cell from which the signals were transmitted. The scanner was mounted underneath a modified DJI S1000 six-copter drone, shown in Fig. 1. The measurement antenna - a dipole multi-band antenna - can be seen extending above the drone chassis. Slightly below, with the white top, is the GNSS antenna for the drone Inertial Measurement Unit (IMU). All measurement recording was time synchronized with the IMU which provided very accurate position information to reference the measurements in 3D space.

At each measurement location, the drone flew along straight street segments of up to 120m in length, depending on the possibilities at the exact location. After take-off, the drone was manually positioned at the lowest height, after which a pre-programmed flight path was initiated. The pre-programmed flight path took the drone along the street at constant height above ground and speed of approximately 2m/s, after which the drone automatically increased the height by nominally 5m. This process was repeated to a maximum height of 35 or 40m, with the drone traversing back and forth along the street segment. Fig. 2 shows an example of the drone flight in one of the measurement locations. In the bottom left corner, the small insert shows how the altitude was increased in a stairway approach, in correspondence with the progression of the pre-programmed flight path.

Each street pass took approximately 60s, which allowed for the collection of an average of 47.5 RSRP/RSRQ sam-

ples per cell. The record of measurement data consists of information relating to numerous cells, i.e. all cells, up to a maximum of 32, for which the synchronization channel was correctly decoded by the scanner; successful detection is achieved if the synchronization channel SINR is above -20dB, and therefore the number of detected cells may vary with the exact propagation conditions at the particular location. Ground level measurements were obtained with an initial drive test inside two of the measurement areas, using the same equipment mounted on top of a passenger car at approximately 2m. Results from this test are included in the path loss modelling as ground level reference. A total of 35 locations, or street segments, were eventually included to the following analysis; results are based either on the area containing most measurement locations (Area 1), or on all three measurement areas. All path loss results are referenced to the line of sight distance to the BSs, based on the 3D position provided by the drone IMU and the BS position information provided by the operators.

III. Results

A. Path Loss Analysis

Using the methodology described in [2], the RSRP measurements reported by the scanner were converted into path loss samples, following Eq. (1), and they represent the frequency averaged received signal power of the LTE reference signal, and therefore a good measure of the local signal strength [7].

$$PL_i[dB] = P_{T_x} + G_a(\theta, \phi) - R_i[dB] \quad (1)$$

P_{T_x} represents the transmitted power per Reference Symbol (RS), G_a is the antenna gain as a function of the azimuth θ and elevation ϕ angle of the drone relative to the antenna boresight direction, and R_i represents RSRP measurements; note, both P_{T_x} and R_i are in units of dBm. Pairs of path loss and line of sight distance (PL_i, d_i) samples were used to fit a log-distance *Close In* (CI) single slope model [8], Eq. (2), using least squares linear regression on distance.

$$PL^{CI}(f,d)[dB] = 20\alpha log_{10}\frac{4\pi f}{c}[dB] + 10\alpha log_{10}\frac{d}{1m}[dB] \quad (2)$$

where $PL^{CI}(f,d)$ is the large-scale path loss at frequency f and distance d, α is the path loss exponent and d is the T_x-R_x line of sight or separation distance. The frequency dependence was verified experimentally in [6].

The path loss model obtained from the new set of measurements is depicted in Fig. 3. A clear decrease of the path loss exponent is observed, from 3.2 at reference level to 2.2 at 40m. For a line of sight distance of 1km, the signal attenuation is approximately 30dB higher at ground level in comparison to 40m.

Additionally, Fig. 4 shows the estimated path loss exponent α and shadowing variation σ versus height, where the latter is calculated from the residuals of the regression in Eq. (2). Corresponding empirical expressions were derived in Eq. (3) and (4) using iterative least square estimations of α and σ on the measurement height.

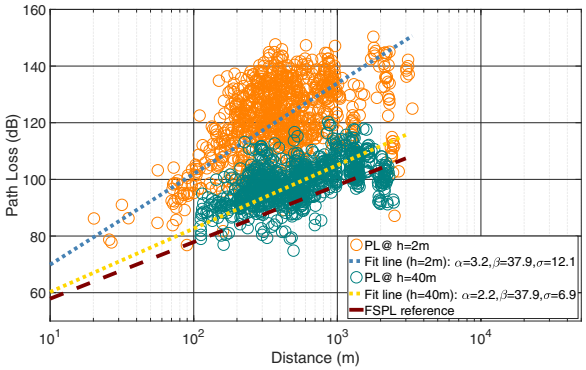

Fig. 3: Path loss slope for ground level reference and 40m.

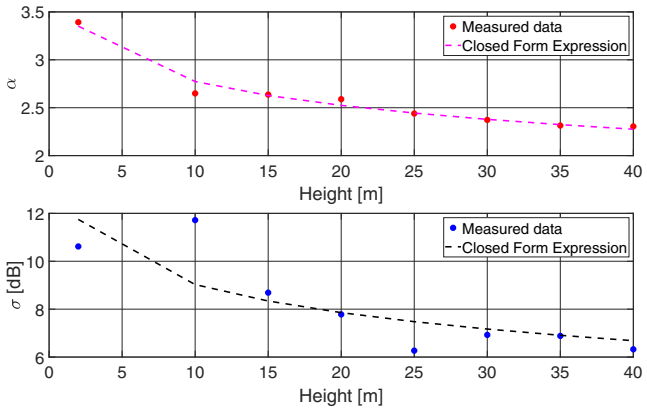

Fig. 4: Height dependent model for the regression parameters α and σ.

$$\alpha(h) = -0.82 \cdot log_{10}(h) + 3.6 \quad (3)$$

$$\sigma(h) = -3.90 \cdot log_{10}(h) + 12.9 \quad (4)$$

These results are consistent with the ones presented in [6] for an urban environment, where similar model parameters have been determined. Considering that the overall behaviour is the same, and that even parameters do not deviate significantly, we find the model to be well supported by empirical evidence. Although the data computed from the measurements are well aligned with the model, we again observe, similar to [6], a deviating behaviour for the shadowing variation at or around rooftop level (10m in Fig. 4), where the standard deviation is above the model prediction. As the results for correlation will show later, propagation at or around rooftop level is more complicated than what can be captured in this simple model. It serves, however, to show the general trends.

B. Interference Analysis

An immediate consequence of the radio clearance is that the drone can detect an increased number of interfering signals coming from BS cells located at longer distances [9], [10]. Fig. 5 displays the average number of cells detected per measurement sample. The results clearly show that elevated

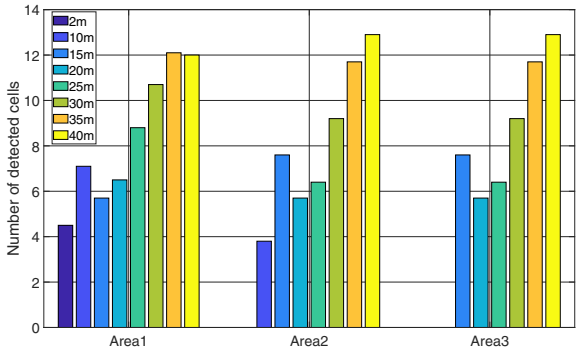

Fig. 5: Average number of detected cells.

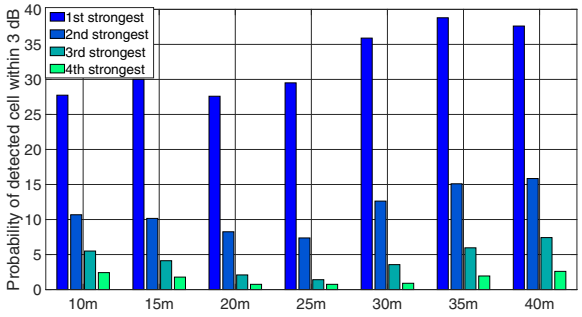

Fig. 6: Number of detected neighbour cell with measured RSRP within a 3 dB threshold.

heights provide a higher number of potential serving cells, which also implies an increase in the number of interfering cells starting from 10m. This trend continues to the highest altitude, where the scanner can detect up to 13 cells in average. Due to the scanner limitation regarding the SINR threshold for detection, and the relative signal level of the strongest versus weak(er) cells, many more cells are likely to go undetected. The observed behaviour was also documented in [9], [10] and [11].

If interfering signals coming from other cells are close in power level to the strongest cell, then interference cancellation at the (drone) terminal may become difficult. In order to assess this effect, Fig. 6 shows the distribution of 1^{st}, 2^{nd}, 3^{rd} and 4^{th} strongest cells, with a signal power within a -3 dB range from the strongest cell power level: for every sample instant, the cell ID that reported the highest measured RSRP level was selected as the reference, and the number of other cells with RSRP level within 3dB of that reference was ordered according to 1^{st}, 2^{nd}, 3^{rd} and 4^{th} strongest cell. As it can be observed from Fig. 6, it is very likely to have one cell within 3dB of the strongest, and also two cells. This is particularly remarked when the drone is well above the average rooftop level, where also the number of sample instants with three and four cells within 3dB starts to become significant. From lowest level to the highest altitude, the number of 1^{st} strongest cells increases by 10 percent points, while for the 2^{nd} there is an increase of 5 percent points.

RSRQ samples were also extracted, and analysis showed that RSRQ has the same behaviour. A consequence of the significant increase in the number of stronger cells, besides the challenges for interference cancellation, is a poor selection of a new serving cell, which can lead to a high number of ineffective handovers. The potential of a number of technical solutions, particularly for coping with the interference challenge, was addressed in [10] and in [11].

C. Correlation analysis

The analysis of the spatial correlation of the shadowing reveals information about its variability along the flight path (laterally) and with height (vertically). The typical measure for the lateral correlation is the *'decorrelation distance'*, which is the distance at which the normalized auto-correlation has decreased to $1/e$ (e being Euler's number). For the vertical correlation, due to limited spatial resolution, we have used the cross-correlation coefficient between the shadowing variability at different heights to characterize the vertical correlation.

The following results are based on RSRP measurements in Area 1. From all the cells detected by the scanner, the analysis was based on the strongest cell within the set of top 3 cell IDs that were most frequently detected by the scanner within a flight duration. The strongest cell was chosen at the lowest flight height, and data for all other heights was subsequently selected accordingly.

Since the shadowing concerns the variations around the local mean level, we first compensated the RSRP measurements for the distance dependent path loss, based on the path loss exponents presented in Section III.A, and second, detrended the distance compensated RSRP values to remove any local mean offset. Compared to the large-scale shadowing analysed in Section III.A, in which samples from the full measurement area were included, we will refer here to local shadow fading since the analysis is per street, and thus represents a far smaller area.

To reduce the impact of any residual fast fading and noise in the measurement data, the distance compensated and detrended RSRP values, were averaged over intervals of approximately 6m. Note, this is in addition to the frequency averaging on the measured RSRP itself.

Decorrelation distance

Fig. 7 shows one example of the normalized auto-correlation function calculated from the averaged RSRP values (un-biased estimate). Also shown, is the first order autocorrelation model suggested by ITU [12]:

$$R(\Delta x) = e^{-\frac{|\Delta x|}{d_{corr}}} \tag{5}$$

where Δx is the distance lag measured along a street segment and d_{corr} the decorrelation distance.

Based on fitting this first order model to the empirically derived unbiased estimate, we obtain the decorrelation distance d_{corr}. The example in Fig. 7 is representative of the fitting that

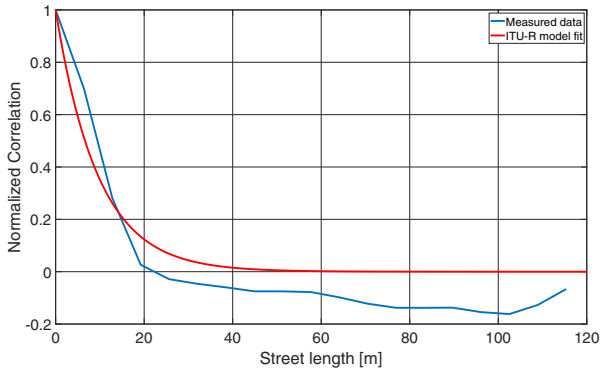

Fig. 7: Example of normalized autocorrelation function in one measured location for one particular cell ID.

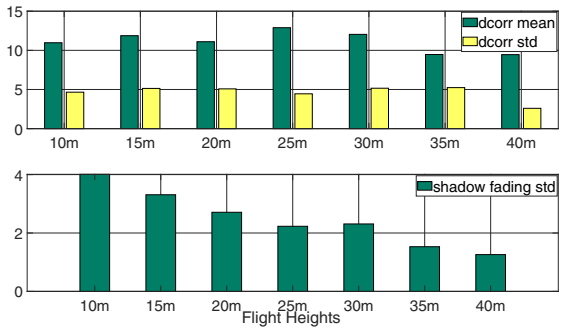

Fig. 8: Top: Decorrelation distance - mean and standard deviation; Bottom: Shadow fading standard deviation.

was obtained in all analyzed street segments, and is generally well in accordance with the first order (autoregressive) model.

Fig. 8 shows the mean and standard deviation of the decorrelation distance, and the shadow fading standard deviation, for all analyzed street segments in Area 1. It is clear, as expected, that the standard deviation obtained for the local shadowing is much lower in comparison to the shadowing standard deviation obtained from analyzing the variation over the larger urban area (Fig. 4). However, the trends are the same.

From the decorrelation results, there is no clear trend with height, as indicated by both the trend in the mean decorrelation distance and the relatively high standard deviation on the estimates. The decorrelation distance is between 9.5 and 12.9m, which corresponds to results reported in [13] and [14] for ground level in urban area. From expectation, the decorrelation distance should increase when the drone gets above rooftop level, due to the clear line of sight to the BSs (free space propagation). A tempting conclusion therefore, in view of the decreasing standard deviation of the shadow fading, could be that different noise effects tend to decorrelate the shadowing with increasing height. That is indeed one explanation, but there is also reason to believe that because of the ground optimized infrastructure, the drone will experience considerable shadow variation due to the side lobes of the BS sector antennas. Typically, the vertical beamwidth is very narrow, in the order of some 10 degrees for a sector antenna, which in combination with the downtilt, gives rise to considerable modulation of the signal when the drone crosses different pattern cuts of the antennas 3D radiation pattern. It remains for further investigation to clarify the exact reason for the observed behaviour.

Cross-correlation

For the vertical correlation, the cross-correlation coefficient was calculated between the averaged RSRP values at different heights. Fig. 9 summarizes the results, by displaying the distribution of the aggregate set of RSRP values on the diagonal, and scatter plots of corresponding RSRP value pairs for respective heights on the off-diagonal. On the scatter plots, we have further indicated the least squares regression line, whose slope - the cross-correlation coefficient - is written next to the scatter plot. The aggregate data sets have symmetric single mode distributions, with standard deviations as per Fig. 8. For the cross-correlation coefficient, it is noticeable that they appear more or less in three distinct groups: Below rooftop (triangle framed in red, upper left) with some trend of having correlation in the shadowing variation at different heights; Above rooftop (triangle framed in yellow, lower right) with no correlation; and finally, Below-to-above rooftop (square framed in green, lower left), also with no correlation between shadowing at different heights.

Below rooftop, propagation is a combination of street guided and over the rooftop propagation - mechanisms which remain more or less the same as long as one stays below rooftop. Above, considering that the previous assumption of significant impact from the vertical antenna side lobes holds, this could lead to fast decorrelation of the shadowing, and therefore explain the observed uncorrelatedness. Further, such an effect can also be claimed independent of below rooftop effects, since they have different origin. As already stated, there is a need for further investigation, especially since there can be other explanations such as the impact of random noise sources (residual fast fading, measurement errors, measurement quantization, etc.), which starts to impact when the standard deviation gets low (viz. trend in Fig. 8).

IV. Conclusions

New and more extensive measurements have confirmed the validity of previously presented modelling frameworks for the path loss behaviour versus height for the drone to cellular infrastructure propagation channel in urban environments. The new measurements have embraced a heterogeneity of base station deployment configurations, drone flight paths and surrounding environments, all contributing to the statistical significance of the results. The results also confirm previous findings on the interference environment that drone communication will experience in an urban environment with high cell density, including an increased number of interfering and/or interfered cells and more dominant interferers. The implications thereof need to be carefully studied, given the impact it can have to

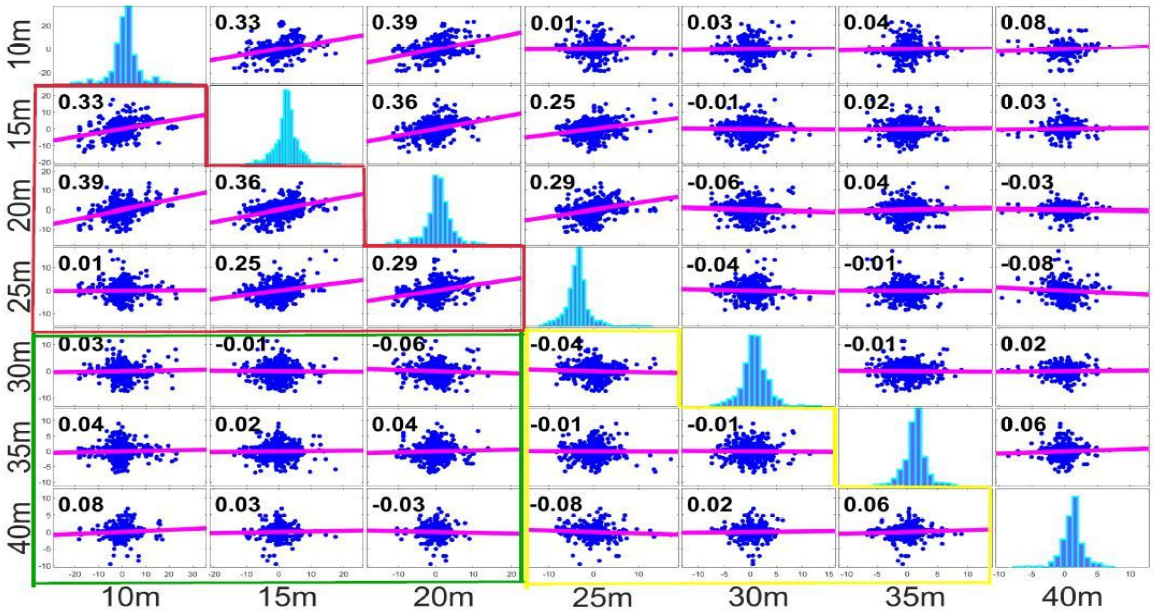

Fig. 9: Correlation matrix overview for all measured heights for Area 1 and Operator 1.

the performance of interference cancellation mechanisms, cell (re-)selection and handover.

Our paper also contributed to better understanding the shadowing variability with height, which is a topic that has not received much attention in the literature so far. Results have been presented for both the lateral decorrelation distance, and the cross-correlation coefficient for the vertical shadowing variability. The decorrelation distance does not appear to change appreciably from ground level up to above rooftop level, and the cross-correlation versus height is generally low. For the latter, however, there is a trend that shadowing is correlated below roof-top level, but not above, nor between below and above rooftop level. In the paper, we have speculated that the vertical side lobes of the base station antennas can have impacted the result, but further analysis is needed for a better understanding of the combined effects of antenna directivity and propagation characteristics of shadow fading. The use of intelligent ray-tracing with accurate 3D city models could be useful to this end.

ACKNOWLEDGMENT

This research was founded by SESAR Joint Undertaking under the European Union's Horizon 2020 research and innovation programme, grant agreement No. 763601.

REFERENCES

[1] SESAR Joint Undertaking, *"U-Space Blueprint brochure"*, Manuscript completed in 2017, Publications Office of the European Union, Luxembourg, 2017.

[2] R. Amorim, H. Nguyen, P. Mogensen, I. Z. Kovács, J. Wigard and T. B. Sørensen, *"Radio Channel Modeling for UAV Communication Over Cellular Networks"*, IEEE Wireless Communications Letters, vol. 6, no. 4, pp. 514-517, August 2017.

[3] 3GPP, *"Enhanced LTE support for aerial vehicles"*, 3GPP, Tech. Rep. TS 36.777, V15.0.0, January 2018.

[4] K. Welch, *"Evolving cellular technologies for safer drone operation"*, Qualcomm 5G White Paper Presentation, San Diego, CA, USA, Tech. Rep., October, 2016.

[5] 3GPP, *"Study on channel model for frequencies from 0.5 to 100 GHz"*, 3GPP, Tech. Rep. TS 38.901, V14.3.0, January 2018.

[6] R. Amorim, H. Nguyen, J. Wigard, I. Z. Kovács, T. B. Sørensen and P. Mogensen, *LTE radio measurements above urban rooftops for aerial communications*, 2018 IEEE Wireless Communications and Networking Conference (WCNC).

[7] 3GPP, *"Evolved Universal Terrestrial Radio Access (E-UTRA); Physical channels and modulation"*, 3GPP, Tech. Rep. TS 36.211, V.8.9.0, 2010-03.

[8] S. Shu, T. Thomas, T.S. Rappaport, H. Nguyen, I. Kovács, I. Rodriguez Larrad, *"Path Loss, Shadow Fading and Line-Of-Sight Probability Models for 5G Urban Macro-Cellular Cells"*, 2015 IEEE Globecom Workshops (GC Wkshps), pp. 1-7, December 2015.

[9] B. V. Der Bergh, A. Chiumento and S. Pollin, *"LTE in the sky: trading off propagation benefits with interference costs for aerial nodes"*, IEEE Communications Magazine, vol. 54, no. 5, pp. 44-50, May 2016.

[10] M. M. Azari, F. Rosas, A. Chiumento, S. Pollin, *"Coexistance of Terrestrial and Aerial Users in Cellular Networks"*, 2017 IEEE Globecom Workshops (GC Wkshps), pp. 1-6, December 2017.

[11] I. Kovacs, R. Amorim, H. C. Nguyen, J. Wigard and P. Mogensen, *"Interference Analysis for UAV Connectivity over LTE Using Aerial Radio Measurements"*, 2017 IEEE 86th Vehicular Technology Conference (VTC-Fall), Toronto, ON, 2017, pp. 1-6.

[12] ITU-R Rec. P.1816: *"The prediction of the time and the spatial profile for broadband land mobile services using UHF and SHF bands"*.

[13] T. B. Sorensen, *"Correlation model for slow fading in a small urban macro cell"*, 9th IEEE International Symposium on Personal, Indoor and Mobile Radio Communications, Boston, MA, USA, pp. 1161-1165 vol.3, 1998.

[14] A. Bttcher, P. Vary, C. Schneider, R. S. Thom, *"De-correlation distance of the large scale parameters in an urban macro cell scenario"*, 6th European Conference on Antennas and Propagation (EUCAP), pp. 1417-1421, Prague, 2012.